Hydrogen evolution reaction mediated by an all-sulfur trinuclear nickel complex

Cyril Pieri, Anirban Bhattacharjee, Alexandre Barrozo, Bruno Faure, Michel Giorgi, Jennifer Fize, Marius Réglier, Martin Field, Maylis Orio, Vincent Artero, et al.

▶ **To cite this version:**

Cyril Pieri, Anirban Bhattacharjee, Alexandre Barrozo, Bruno Faure, Michel Giorgi, et al.. Hydrogen evolution reaction mediated by an all-sulfur trinuclear nickel complex. Chemical Communications, 2020, 56 (75), pp.11106-11109. 10.1039/d0cc04174b . hal-02961657

HAL Id: hal-02961657
https://hal.science/hal-02961657

Submitted on 17 Nov 2020

HAL is a multi-disciplinary open access archive for the deposit and dissemination of scientific research documents, whether they are published or not. The documents may come from teaching and research institutions in France or abroad, or from public or private research centers.

L'archive ouverte pluridisciplinaire **HAL**, est destinée au dépôt et à la diffusion de documents scientifiques de niveau recherche, publiés ou non, émanant des établissements d'enseignement et de recherche français ou étrangers, des laboratoires publics ou privés.

COMMUNICATION

Hydrogen evolution reaction mediated by an all-sulfur trinuclear nickel complex

Received 00th January 20xx,
Accepted 00th January 20xx

DOI: 10.1039/x0xx00000x

Cyril Pieri,[a] Anirban Bhattecharjee,[b] Alexandre Barrozo,[a] Bruno Faure,[a] Michel Giorgi,[c] Jennifer Fize,[d] Marius Réglier,[a] Martin Field,[d]* Maylis Orio,[a]* Vincent Artero[d] and Renaud Hardré [a]*

We report the synthesis and the characterization of a trinuclear nickel complex. Solid state and solution studies using X-ray diffraction, NMR and UV-vis spectroscopy highlight the square planar geometries around the metal centers and an all-sulfur coordination sphere. It exhibits significant electrocatalytic activity for hydrogen evolution in DMF using Et_3NHCl as the proton source. The theoretical reaction mechanism suggests that sulfur atoms act as proton relay, as proposed in [NiFe] hydrogenases.

The limited sources of fossil fuels, together with their environmental impact, render them unviable in the long run. This is aggravated by an increasing energy demand worldwide, resulting in higher prices, as well as with the lack of renewability of fossil energy at the human time scale.[1] To the contrary, dihydrogen seems to be an ideal substitute, since it is based on the most abundant atom in the universe, and its combustion yields high energy, with water as the only waste.[2,3] The main issue remains with its production. While water electrolysis appears as the most efficient way to produce hydrogen, the flexible proton exchange membrane technology requires the use of platinum, a rare and expensive metal with limited stocks.[4] In the search for an economically competitive way of producing dihydrogen with non-noble metal-based catalysts, Nature can guide us and inspiration can be found with the [NiFe] hydrogenases. This family of enzymes is a very attractive example as it is the most abundant hydrogenases among living organisms. Their active sites are composed of two metal ions, iron and nickel, the latter lying in a rare all-sulfur and distorted tetrahedral coordination geometry.[5-7] Many bio-inspired complexes mimicking this active site can be found in literature[8-15] These models generally show some degree of variation from the enzyme active site: metals, coordinating atoms, bridging and exogenous ligands, *e.g.* CO and CN^-.[16-18] To reproduce the features of the [NiFe] hydrogenase active site, an all-sulfur nickel complex was obtained by Yamamura *et al*. in 1985, long before the crystal structure of the enzyme was resolved.[19] Sellman *et al*. also explored a certain number of all-sulfur nickel complexes.[20] Once the structure of the [NiFe] hydrogenase was known, many heterobimetallic complexes were then developed.[21] Unlike the enzyme, all of these complexes suffered from a lack of nickel centred reactivity[22] and the situation only changed recently.[12, 23-28] Moreover, the hydrogen producing catalytic performances of these complexes with respect to overpotential requirement and turnover frequency (TOF) towards hydrogen production were far below those of [NiFe] hydrogenases, operating at the thermodynamic equilibrium with a TOF around 1,000 s^{-1}.[29,30] The high activity of hydrogenase depends on the presence of proton relays at the vicinity of the active site. In [NiFe] hydrogenases, terminal cysteinates have been assigned this role.[22] While there are several examples of FeFe hydrogenase models with terminal thiolate ligands prone to protonation,[31,32] there is only one known example of a NiFe complex, and this was only observed under strongly acidic conditions, not pertinent for catalysis.[33] In this context, we have developed a bio-inspired nickel complex bearing an all-sulfur and constrained ligand that resembles the Ni-center of the enzyme active site with its cysteine-thiolate ligands implicated as bases in proton transfer reactions.

Inspired by the seminal work of Bosnich and Pickett,[34-36] our strategy to prepare the trithiol **3** was to start the synthesis from the thiol **1** easily accessible according to the Bosnich procedure.[34, 37] Compound **2** was then obtained by *S*-alkylation of **1** with 2-bromoethyl-trityl-sulfide. Removal of the trityl substituent in dry acidic condition (CF_3COOH) and the reduction of the disulfide moiety by triethyltin hydride led to the trithiol **3**. This overall process provided access to the trithiol **3** which was used for the synthesis of Ni(II) complexes. Thus, the reaction of the ligand **3** with 1 eq. of $[Ni(CH_3CN)_6](BF_4)_2$ in acetonitrile with K_2CO_3 as base led to the formation of a soluble complex that rapidly evolved by the formation of a brown precipitate. Filtration followed by liquid chromatography with CH_2Cl_2 as eluant allowed us to get the pure Ni(II) complex **4** in 45% yield (Scheme 1).

Suitable crystals were obtained from a saturated solution of the complex in CH_3CN. The complex crystallizes as a symmetric trimer with the central Ni-atom lying on the crystallographic two-fold axis (Figure 1).

[a] Aix Marseille Univ, CNRS, Centrale Marseille, iSm2, Marseille, France. E-mail: renaud.hadre@univ-amu.fr, maylis.orio@univ-amu.fr
[b] Socivolta Inc., 3 Place Ville Marie, suite 400 Montreal, QC H3B 2E3, Canada
[c] Aix Marseille Univ, CNRS, Centrale Marseille, Spectropole FR1739, Marseille, France
[d] Univ. Grenoble Alpes, CNRS, CEA, IRIG, Laboratoire de Chimie et Biologie des Métaux, 17 rue des Martyrs, 38000 Grenoble, France. E-mail: martin.field@cea.fr

Please do not adjust margins

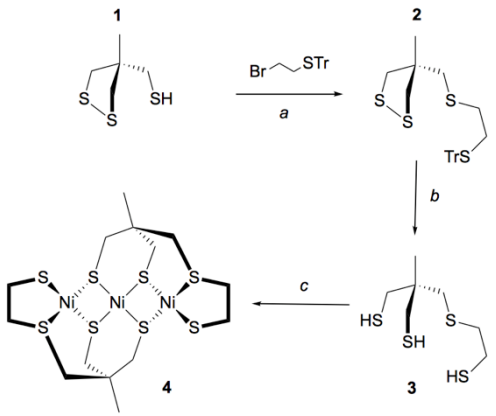

Scheme 1 Synthetic route for the nickel complex **4**. Conditions: a) NaH, THF, 0°C to RT, overnight, 66%; b) CF_3COOH (excess), Et_3SiH (3 eq), CH_2Cl_2, RT overnight, 81%; c) $[Ni(CH_3CN)_6](BF_4)_2$, K_2CO_3 (3 eq), CH_3CN, RT, 2h.

The asymmetric unit is thus composed of half the complex. The coordination geometries of the metals are square planar with small deviations from planar (defined by the Ni and the four coordinated S atoms, Figure S6 and Table S1): the maximum out-of-plane distances are close to 0.15 Å and 0.19 Å (S1 in plane P1 including Ni2 and S1 in plane P2 including Ni1, respectively). The dihedral angle between P1 and P2 is equal to 73.0697(4)°, while the dihedral angle between P1 and the symmetric plane P1' (symmetry code ': 1-x, y, 3/2-z) is equal to 33.8471(8). The structure of compound **4** is therefore very compact and folded with a bowl shape and a small accessible cavity toward the central Ni-atom (mean width and depth equal to 3.4 Å and 4.9 Å, respectively, Table S2).

To check that the structure of **4** corresponds to the one found in solution, we performed the UV-vis titration of the ligand **3** by nickel perchlorate in the presence of triethylamine in DMF. Upon addition of $[Ni(H_2O)_6](ClO_4$, the UV-vis spectrum displays three absorption bands at 290 nm, 410 nm and 540 nm (Figure S3).

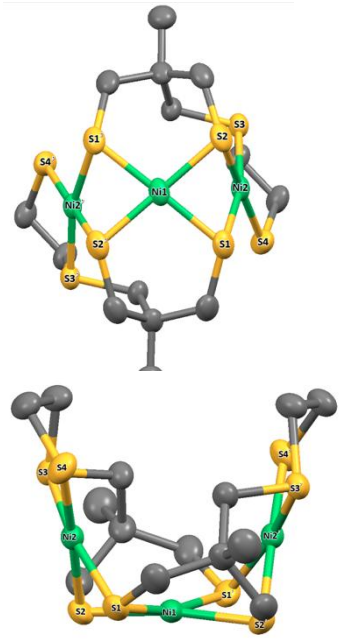

Figure 1 X-ray molecular structure of **4** with atom labelling scheme and ellipsoid parameters at 50% probability level. Hydrogen atoms and carbon labels are omitted for clarity.

Plotting the molecular extinction coefficient as a function of the number of Ni(II) equivalents for each absorption band allowed us to determine the stoichiometry of the complex (Figure S4). Analysis of the titration curves for both the 410 and 540 nm bands support the formation of a trinuclear species like **4** with a 2:3 nickel to ligand ratio, *e.g.* 2 ligands for 3 metal ions.

To support the above assignment, we used time-dependent DFT to calculate the theoretical UV-Vis spectrum of **4** (Figure S9 and Table S5) in the trimer form revealed by X-ray diffraction. Our computations support that its UV-vis spectrum is dominated by three main absorption bands of different intensity (Figure S10). The low-energy absorption is assigned to a d-d transition while the two other spectral features are attributed to charge transfers from the ligand to metal (Figure S11 and Table S4). Both the shape and relative intensities of the calculated spectrum are in pretty fair agreement with the spectrum measured in solution.

The electrochemical study of **4** was performed by cyclic voltammetry between +0.5 and –2.5 V *vs.* $Fc^{+/0}$ (Figure 2). In the cathodic region, two one-electron redox systems were observed: one quasi-reversible at –1.65 V (½(E_{pc}*+E_{pa}*)) and another irreversible at –2.09 V *vs.* $Fc^{+/0}$ (E_{pc}**). The plot of the peak current versus the square root of the scan rates for the reversible cathodic wave was found to be linear, indicating that it is a diffusion-controlled process (Figure S7). In the anodic direction, the CV revealed one oxidative process with an irreversible wave observed at +0.22 V *vs.* $Fc^{+/0}$.

In an effort to gain insight into the nature of the species observed during cyclic voltammetry experiments, we calculated the structures of the putative species resulting from one and two-electron reduction of **4** (Figures S12-14 and Tables S6-8), and their electronic properties. Upon reduction,

This journal is © The Royal Society of Chemistry 20xx

Please do not adjust margins

our results indicate that most of the spin density is distributed at one nickel center (Figure S15). The first reduction process of **4** occurs at the central metal site leading to the formation of a Ni(II)-Ni(I)-Ni(II) complex. The two-electron reduction of **4** results in a triplet ground spin state S = 1 with a stabilization energy of 24 kJ.mol^{-1} over the singlet state S = 0. This result supports a metal-based reduction occurring on another nickel center (Figure S16) and leading to the formation of a Ni(I)-Ni(II)-Ni(I) complex. We can notice a subsequent electronic rearrangement between the first and second reduction, which explains the irreversibility observed experimentally for the second redox system.

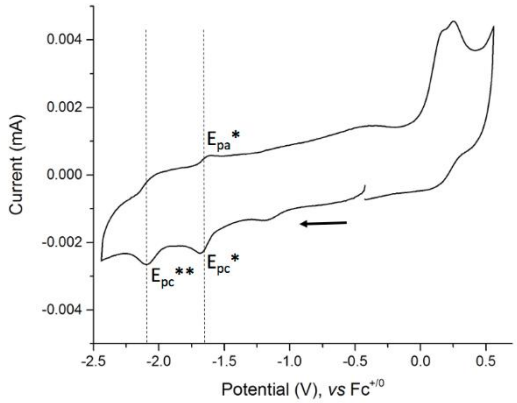

Figure 2 Cyclic voltammogram of **4**, concentration 0.3 mM at a stationary glassy carbon electrode (3 mm diameter) in DMF + 0.1M NEt_4ClO_4. Scan rate 100 mV.s^{-1}.

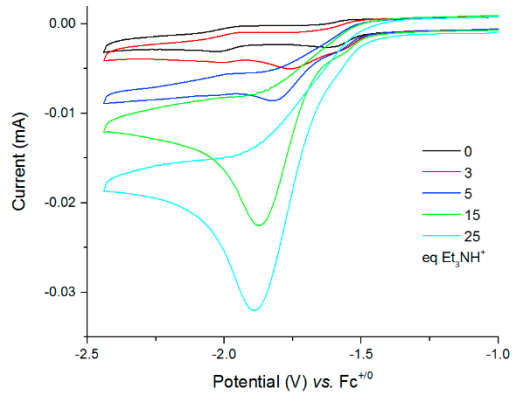

Figure 3 Cyclic voltammograms of a 0.25 mM solution of **4** in DMF (0.1 M NEt_4ClO_4) with increasing amounts of Et_3NHCl (0-55 equiv.) recorded at a glassy carbon electrode (3 mm diameter) and 100 mV.s^{-1}.

Redox potential calculations were conducted to fully assign the electrochemical events (Tables SI-3). The computed values for the one- and two-electron reduction processes are in good agreement with experiment which indicates that the two cathodic systems correspond to a monoelectronic processes. and support the above assignments of the reduction loci in **4**.

To examine the capability of complex **4** to mediate proton reduction catalysis, its electrochemical behaviour was studied by cyclic voltammetry in the presence of Et_3NHCl (pK_a = 9.2in DMF)[38,39] as proton source. Cyclic voltammograms of **4** were recorded under argon in DMF solutions with increased amounts of Et_3NHCl (Figure 3) and show a large irreversible catalytic wave with a mid-wave potential E^0_{cat} of –1.70 ± 0.03 V *vs.* $Fc^{+/0}$, *i.e.* close to the reduction potential of **4**. The current response of this peak-shaped wave is directly proportional to the concentration of protons in the electrolyte solution (Figure S8). A value of 590 mV was calculated for the overpotential requirement of **4** for proton reduction in the presence of Et_3NHCl in DMF.[39]

To confirm that the observed catalytic waves correspond to the electrocatalytic reduction of protons into hydrogen, we performed a bulk electrolysis experiment of a DMF solution of Et_3NHCl in excess (200 mM) and **4** (1 mM). Gas products were monitored by continuous in-line GC analysis. A potential of –1.60 V versus $Fc^{+/0}$ was applied to the mercury-pool working electrode resulting in the immediate formation of hydrogen. This experiment rules out the possibility that proton reduction occurs as the result of deposition of nickel nanoparticles on the electrode surface since they would amalgamate within the mercury pool electrode. Consequently, under these conditions catalysis mediated by **4** is expected to be homogeneous in nature. During the 15 h experiment, a turnover number of 5 was achieved with a moderate Faradaic yield of 30%; indicating some degradation of the complex during turn-over.

DFT calculations were finally conducted to decipher the reaction mechanism of hydrogen evolution by **4** (Scheme 2). We propose the catalytic cycle for H_2 evolution presented in Scheme 2 and based on the ECEC sequence, classically found for cobalt and nickel complexes.[40-42] UV/Vis measurements performed in the absence and presence of Et_3NHCl (Figure SI-5) display almost identical features, indicating that the structure of **4** is unaffected by the addition of a proton source of such strength. From the cyclic voltammetry measurements in the presence of acid, it can be inferred that the reaction proceeds from the one-electron reduced species with a midwave electrocatalytic potential equal to that of the first reduction in **4** denoted [Ni_3'$S4'_2$]. The first reduction at the Ni site was calculated at potentials of –1.84 and –2.02 V vs $Fc^{+/0}$ when using the B86 and B3LYP functionals, respectively (Table S3). We then investigated the protonation of the reduced complex [$Ni'_3S4'_2$]$^-$ with Et_3NH^+ yielding [HNi_3'$S4'_2$]. Two distinct protonation sites could be found. The most stable isomer (by 28 and 61 kJ/mol^{-1} with BP86/B3LYP, respectively) is protonated on a terminal thiolate ligand coordinated on a peripheral Ni ion that remains in a square-planar environment (Figure S17 and Table S9). This reaction is calculated to be almost isergonic. Another isomer, with higher energy, is obtained when protonation occurs at the Ni site thus yielding a hydride derivative with a distorted square-based pyramidal geometry (Figure S18 and Table S10). Reduction of the two isomers of [HNi_3'$S4'_2$] yielding [HNi_3'$S4'_2$]$^-$ is calculated to occur at potentials close to the one calculated for the first reduction of [Ni_3'$S4'_2$]. We note that the stability order of the two isomers is inverted after this reduction step: in that case the sulfur-protonated species (Figure S19 and Table S11) is less stable (by 76 and 24 kJ.mol^{-1} with BP86/B3LY, respectively) than the Ni-hydride square-

Please do not adjust margins

planar isomer (Figure S20 and Table S12) in which one thioether ligand has been eliminated from the Ni coordination sphere and replaced by the hydride ligand.

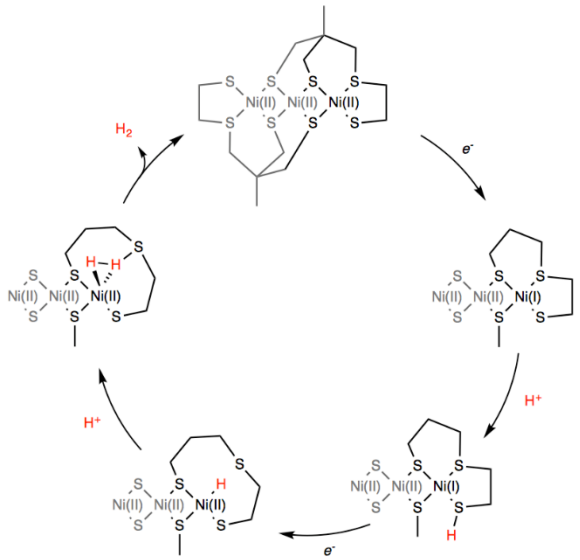

Scheme 2 Proposed DFT computed reaction mechanism for hydrogen evolution mediated by **4**.

Finally, protonation of the reduced hydride species $[HNi_3'S4'_2]^-$ leads to formation of a dihydrogen complex $[(H_2)Ni_3'S4'_2]$ (Figure S21 and Table S13). This reaction is calculated to be thermodynamically favorable. The structure is reminiscent of a dihydrogen bond between nickel and sulfur that has been proposed as a key intermediate in the route to H_2 evolution at the active site of [NiFe] hydrogenases (Ni-R in Scheme 3).[44,45] From this dihydrogen complex, liberation of H_2 is strongly and entropically favored. Removal of H_2 leads to the original structure of $[Ni_3'S4'_2]$ thus closing the catalytic cycle.

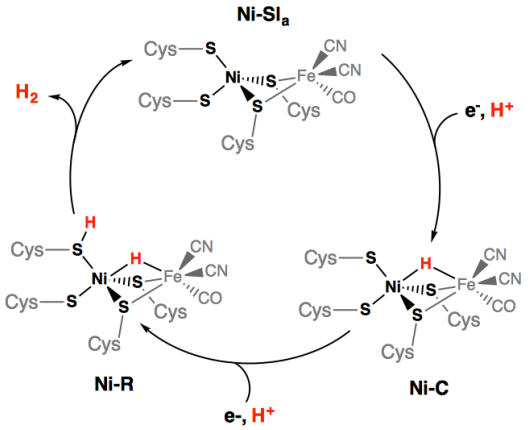

Scheme 3 Catalytic cycle of the [NiFe] hydrogenases involving the Ni-SIa, Ni-R, and Ni-C states.

In this work, we have reported the experimental and theoretical study of an original trinuclear nickel complex that displays an all-sulfur coordination sphere and exhibits a significant catalytic activity with a moderate overpotential requirement for hydrogen production in DMF using Et_3NHCl as the proton source. Detailed analysis of the electrocatalytic data combined with DFT calculations allowed us to propose an ECEC catalytic pathway involving Ni-bound terminal thiolate ligand as proton relay mimicking the role of terminal cysteinate ligand in the active site of [NiFe] hydrogenases. Further work is currently in progress in our group to develop new bio-inspired mimics of the [NiFe] hydrogenase and to design original polynuclear metal complexes with thiolate ligands capable of mediating efficient hydrogen evolution.

Conflicts of interest

There are no conflicts to declare.

Acknowledgements

The authors gratefully acknowledge research support of this work by the French National Research Agency (CODEC, ANR-19-CE05_0030_01; $CatH_2$, ANR-07-BLAN-0298; NiFe-Cat, ANR-2010-BLAN-711-1; NiFemim, ANR-DFG-2016-NLE; Labex ARCANE; Graduate school of Chemistry, Biology and Health of Univ. Grenoble Alpes, CBH-EUR-GS, ANR-17-EURE-0003).

Notes and references

1 D. A. King, *Science*, 2004, **303**, 176.
2 J. A. Turner, *Science*, 2004, **305**, 972.
3 P. P. Edwards, V. L. Kuznetsov, W. I. F. David, N. P. Brandon, *Energy Policy*, 2008, **36**, 4356.
4 J. R. McKone, S. C. Marinescu, B. S. Brunschwig, J. R. Winkler, H. B. Gray, *Chem. Sci.* 2014, **5**, 865.
5 A. Volbeda, M-H. Charon, C. Piras, E.C. Hatchikian, M. Frey, J-C. Fontecilla-Camps, *Nature*, 1995, **373**, 580.
6 A. Volbeda A, E. Garcin, C. Piras, A. L. de Lacey, V.M. Fernandez , E.C. Hatchikian, M. Frey, J-C. Fontecilla-Camps, *J. Am. Chem. Soc.*, 1996, **118**, 12989.
7 R.P. Happe, W. Roseboom, A.J. Pierik, S.P.J Albracht, K.A. Bagley, *Nature* 1997, **385**, 126.
8 D. Sirbu, T. Straistari, A. C Benniston, Hydrogenases: From Biomimetic to Bioinspired Models in *Bioinspired Chemistry, From Enzymes to Synthetic Models*, 2019, **5**, 89.
9 T. B. Rauchfuss, Acc. Chem. Res., 2015, **48**, 2107.
10 M. Y. Darensbourg, E.J. Lyon, J.J. Smee, Coord. Chem. Rev., 2000, **206**, 533.
11 Z. Li, Y. Ohki, K. Tatsumi, J. Am. Chem. Soc., 2005, **127**, 8950.
12 D. Brazzolotto, M. Gennari, N. Queyriaux, T.R. Simmons, J. Pecaut, S. Demeshko, F. Meyer, M. Orio, V.Artero, C. Duboc, Nat. Chem., 2016, **8**, 1054.
13 S. Canaguier, M. Field, Y. Oudart, J. Pécaut, M. Fontecave, V. Artero, Chem. Comm., 2010, 46, 5876.
14 D. Basu, T. Spencer Bailey, Noémie Lalaoui, Casseday P. Richers, Toby J. Woods, Thomas B. Rauchfuss, Federica Arrigoni, Giuseppe Zampella, *Inorg. Chem.* 2019, **58**, 4, 2430.
15 N. Coutard, N. Kaeffer, V. Artero, *Chem. Commun.*, 2016, **52**, 13728.
16 A. C. Marr, D. J.E. Spencer, M. Schröder, *Coord. Chem. Rev*. 2001, **219–221**, 1055.

This journal is © The Royal Society of Chemistry 20xx

Please do not adjust margins

Please do not adjust margins

17 T. R. Simmons, G. Berggrena, M. Bacchi, M. Fontecave, V. Artero, *Coord. Chem. Rev*., 2014, **270-271**, 127.
18 E. Bouwman, J. Reedijk, *Coord. Chem. Rev*., 2005, **15-16**, 1555.
19 T. Yamamura, H. Miyamae, Y. Katayama, Y. Sasaki, *Chem. Lett.*, 1985, 269.
20 D. Sellmann, S. Fünfgelder, G. Pohlmann, F. Knoch, M. Moll, *Inorg. Chem.*, 1990, **29**, 23, 4772.
21 S. Kaur-Ghumaan, M. Stein, *Dalton Trans.*, 2014, **43**, 9392
22 W. Lubitz, H. Ogata, O. Rüdiger, E. Reijerse, *Chem. Rev.,* 2014 **114**, 4081.
23 H. Tang, M. B. Hall, *J. Am. Chem. Soc.*, 2017, **139**, 18065.
24 D. Brazzolotto, L. Wang, H. Tang, M. Gennari, N. Queyriaux, C. Philouze, S. Demeshko, F. Meyer, M. Orio, V. Artero, M. B. Hall, C. Duboc, *ACS Catal.*, 2018, **8**, 10658.
25 G. M. Chambers, M. T> Huynh, Y. Li, S. Hammes-Schiffer, T.B. Rauchfuss, E. Reijerse, W. Lubitz, *Inorg. Chem.*, 2016, **55**, 419.
26 S. Ding, P. Ghosh, A. M. Lunsford, N. Wang, N. Bhuvanesh, M. B. Hall, M. BY. Darensbourg, *J. Am. Chem. Soc.* 2016, **138**, 12920.
27 S. Ding, P. Ghosh, A. M Lunsford, N. Wang, N. Bhuvanesh, M. B. Hall, M. Y. Darensbourg, *J. Am. Chem. Soc.* 2016, **138**, 12920.
28 S. Ding, P. Ghosh, M. Y.Darensbourg, M. B.Hall, *Proc. Natl. Acad. Sci.*, 2017, **114**, E9775.
29 M. E. Ahmed, A. Dey, *Curr. Opin. Electrochem.,* 2019, **15**,155
30 D. Schilter, J. M. Camara, M. T. Huynh, S. Hammes-Schiffer, T. B. Rauchfuss et al, *Chem. Rev.*, 2016, **116**, 8693.
31 U-P. Apfel, D. Troegel, Y. Halpin, S. Tschierlei, U. Uhlemann, H. Görls, M. Schmitt, J. Popp, P. Dunne, M. Venkatesan, M. Coey, M. Rudolph, J. G. Vos, R. Tacke, W. Weigand, *Inorg. Chem* 2010, **49**, 21, 10117.
32 R. Zaffaroni, T. B. Rauchfuss, D. L. Gray, L. De Gioia, G. Zampella, *J. Am. Chem. Soc.* 2012, **134**, 46, 19260.
33 Lubitz (1) Weber, K.; Krämer, T.; Shafaat, H. S.; Weyhermüller, T.; Bill, E.; van Gastel, M.; Neese, F.; Lubitz, W. *J. Am. Chem. Soc.* 2012, **134**, 20745.
34 C. Kolomyjec, J. Whelan, B. Bosnich, *Inorg. Chem*., 1983, **22**, 2343.
35 M. Razavet, S. C. Davies, D. L. Hughes, C. J. Pickett, *Chem. Commun.*, 2001, **847**.
36 M. Razavet, S. C Davies, D. L. Hughes, J. E. Barclay, D. J. Evans, S. A Fairhurst, X. Liu, C. J. Pickett, *Dalton Trans*, 2003, **586**.
37 R. A. Valiulin, A. G Kutateladze, *J. Org. Chem.*, 2008, **73**, 335.
38 K. Izutsu, Acid-Base Dissociation Constants in *Dipolar Aprotic Solvents*; 1990**,** Blackwell Scientific: Oxford, U.K.
39 V. Fourmond, P.-. Jacques, M. Fontecave, V. Artero, *Inorg. Chem*., 2010, **49**, 10338.
40 V. Artero; J.-M. Saveant, *Energy Environ. Sci.*, 2014, **7**, 3808.
41 J. L. Dempsey, B. S. Brunschwig, J. R. Winkler, H. B. Gray, *Acc. Chem. Res.*, 2009, **42**, 1995.
42 N. Kaeffer, M. Chavarot-Kerlidou, V. Artero, *Acc. Chem. Res.*, 2015, **48**, 1286.
43 N. Queyriaux, R.T. Jane, J. Massin, V. Artero, M. Chavarot-Kerlidou, *Coord. Chem. Rev*., 201**5**, **304-30**5, 3.
44 P. E. M. Siegbahn, J. W. Tye, M. B. Hall, *Chem. Rev.*, 2007, **107**, 4414.
45 G. Dong, U. Ryde, *JBIC*, 2016, **21**, 383.

This journal is © The Royal Society of Chemistry 20xx

Please do not adjust margins